N89-10852

GROUND VORTEX FLOW FIELD INVESTIGATION

Richard E. Kuhn
STOVL Consultant
Valencia, California

John H. Del Frate
NASA Ames Research Center
Dryden Flight Research Facility
Edwards, California

and

James E. Eshleman
Lockheed California Co.
Burbank, California

INTRODUCTION

In hover and low-speed operation the jets from a V/STOL configuration impinge on the ground and form a wall jet flowing radially outward from the impingement point of each jet. In STOL operation the forward-flowing part of the wall jet is opposed by the free stream generated by forward motion and is rolled back on itself to form a horseshoe-shaped ground vortex, as shown in figure 1. When operating over loose terrain this ground vortex creates and defines the dust cloud that can reduce visibility and damage engines. It is also one of the primary mechanisms of hot gas ingestion and can cause significant lift loss and associated pitching and rolling (in a sideslip condition) moments.

The flow field associated with the ground vortex formed in STOL operation has been studied in several investigations (refs. 1 to 5). Unfortunately, these five investigations show a wide variation in the forward projection of the ground vortex flow field, as shown in figure 2. Some of this variation may be due to the manner in which the forward edge of the flow field was defined. Some measured the position from photographs of dust clouds and some inferred the position from pressure distributions measured on the ground board. Also they were run at different jet pressure ratios and Reynolds numbers.

However, it is believed that the boundary layer present in most tests between the free stream and the ground board and the relative motion between the jet and the ground surface may be the primary factors responsible for the variations in the forward projection (fig. 2). Most of these investigations were conducted in wind tunnels with fixed ground boards. When using this test technique a boundary layer forms between the free stream and the ground board. The velocity decrement of the ground board boundary layer allows the high-velocity wall jet to penetrate further upstream than would be possible against a full free-stream velocity profile. All the wind tunnel investigations (refs. 1 to 4) show more forward penetration than the moving model investigation (ref. 5), where there was no boundary layer. Also, in the moving model case the ground surface is moving rearward relative to the wall jet flow and therefore retarding and eroding the energy of the wall jet and reducing its ability to penetrate against the free stream.

To avoid the ingestion of hot gas or dirt and debris, the inlet should be ahead of or above the recirculating flow field generated by the ground vortex. Unfortunately, the height of the recirculating flow field has received very little attention. Abbott (ref. 5) simply states that the depth of the flow field is approximately one-half the forward projection. This result was obtained from jet-alone tests. It has been speculated that the sink effect of an inlet, located slightly above or ahead of the ground vortex, may increase the height or forward extent of the flow field. Unfortunately, there have been no investigations of the sink effect of the inlet.

The investigations described in this paper had several objectives:

1. to evaluate water tunnel tests as a technique to visualize and evaluate the flow field under and ahead of a V/STOL model;

2. to investigate the effects of the boundary layer and movement relative to the ground on the forward projection of the flow field;

3. to determine the depth of the flow field;

4. to investigate the effects of inlet flow on the forward extent and depth of the flow field; and

5. to investigate the flow fields generated by twin-jet configurations.

SUMMARY

Flow field investigations were conducted at the NASA Ames-Dryden Flow Visualization Facility (water tunnel) to study the ground vortex produced by the impingement of jets from aircraft nozzles on a ground board in a STOL operation. Effects on the overall flow field with both a stationary and a moving ground board were photographed and compared with similar data found in other references. Additionally, nozzle jet impingement angles, nozzle and inlet interaction, side-by-side nozzles, nozzles in tandem, and nozzles and inlets mounted on a flat plate model were investigated. Results show that the wall jet that generates the ground vortex is unsteady and the boundary between the ground vortex flow field and the free-stream flow is unsteady. Additionally, the forward projection of the ground vortex flow field with a moving ground board is one-third less than that measured over a fixed ground board. Results also showed that inlets did not alter the ground vortex flow field.

NOMENCLATURE

d	jet diameter, ft
h	height of jet exit above ground, ft
K	factor to account for moving ground
m_i/m_j	inlet mass to jet mass flow ratio
q_0	free-stream dynamic pressure, lb/ft^2
q_j	jet dynamic pressure, lb/ft^2
V_0	free-stream velocity, ft/sec
V_j	jet velocity, ft/sec
V_b	belt velocity, ft/sec
w/ℓ	width/length ratio of jet nozzle
X	forward projection of ground vortex flow field, ft
x	longitudinal distance between jet centers in tandem pair, ft

z depth of ground vortex flow field, ft

δ jet deflection angle, measured from horizontal, deg

MODEL AND APPARATUS

The investigation was conducted in the Flow Visualization Facility (ref. 6) at the NASA Ames Research Center, Dryden Flight Research Facility. This flow visualization facility is a continuous-flow water tunnel with a vertical test section (fig. 3). The walls of the 16- by 24-in test section are made of 2-in-thick plexiglass to provide for easy visual and photographic observation of the flow. Photographs can be taken either using general lighting or using a light sheet generated by an argon laser.

The setup for the investigation is shown in figure 4. A special endless-belt ground board was built for these studies. The belt material was transparent plastic, and the belt was supported by a transparent backing plate (in the jet impingement region) so that photographs could be taken and the flow field could be illuminated by the laser light sheet through the belt. The belt assembly was installed against the 16-in side of the tunnel, and fairings were installed upstream and downstream of the belt to ensure smooth flow. A boundary layer removal system was installed at the leading edge of the belt to remove the boundary layer generated on the wall and fairing ahead of the belt. The regeneration of the boundary layer on the belt surface was eliminated by operating the belt at the free-stream velocity.

The investigation was conducted in two phases. Phase I, conducted in September 1986, used a 0.5-in-diameter jet and a 1-in-diameter inlet (fig. 4) in an investigation of the effects of jet/free-stream velocity ratio, belt speed, jet height, jet deflection angle, and inlet flow on the ground vortex flow field set up by the jet. The jet could be positioned at heights from 1 to 5 in. above the ground board. The inlet was supported from the tubing supporting the jet, and both the fore and aft position and the height of the inlet could be varied.

Phase II, conducted in December 1986, extended the investigation to cover the effects of dual jets, side-by-side or in tandem, and the effects of the proximity of a wing or body surface at the exit plane. The clipped delta configuration and the inlet and jet positions and spacings investigated are shown in figure 5.

For the phase II tests, the diameters of the two individual jets were reduced to 0.35 in each. Also, extra precautions were taken in the construction of the phase II nozzles to reduce the turbulence of the jets. As shown in figure 6, the phase II nozzles incorporated two screens and a finer honeycomb than that used in the phase I nozzle.

RESULTS AND DISCUSSION

All the data from the present investigation were obtained from still photographs and video records of the flow. The best insight into the flow is obtained from the video records; a 15-min tape was prepared to illustrate the significant findings of

the study. (This tape is available on loan and can be obtained by contacting John Del Frate at the NASA Ames Research Center, Dryden Flight Research Facility.)

Figure 7 presents a typical still photograph of the flow illuminated by the laser light sheet. In this photograph the jet is at a height of 2 diameters and the inlet is at a moderately high and forward position. This photograph was taken with the jet operating at a velocity 6.1 times the free-stream velocity, no inlet flow, and the belt stopped. The free-stream flow is from right to left. Fluorescent dye was injected into the jet flow well upstream of the nozzle to make the jet flow visible. The impingement of the jet stream on the ground and the formation of the wall jet can be seen.

At this ratio of jet velocity V_j to free-stream velocity V_0 ($V_j/V_0 = 6.1$) the ground vortex flow field is seen to project about 5 jet diameters ahead of the jet center line. However, the boundary between the ground vortex flow field and the free stream is not smooth, as is implied in figure 1, but is very irregular and unsteady. Observations during the test and posttest analysis of the video records show a significant unsteadiness of this boundary with what appear to be chunks of the ground vortex flow field being projected out through the boundary at random intervals and at random positions of the horseshoe-shaped front of the ground vortex flow field. Similar behavior was observed using smoke flow in a related investigation of ground vortex flow fields (ref. 7).

A unique feature of the flow with the belt stopped is the formation of a boundary layer wedge immediately upstream of the ground vortex flow field. This wedge is similar to that observed in the boundary layer of the free stream approaching a step on a flat plate. In the present case there appear to be vortices imbedded in this wedge, and these vortices are rotating in the same direction as the ground vortex. Visualizations and the video records show these vortices peeling off from the wedge and rolling up over the ground vortex flow field.

How much of the unsteadiness of the boundary between the ground vortex flow field and the free stream is associated with the remnants of these vortex-like flows being transported back over the ground vortex flow field cannot be determined. However, the boundary layer wedges are primarily associated with the belt-stopped testing conditions. With the belt running at free-stream velocity, the boundary layer wedge was seldom observed. At times it appeared that a wedge would form; however, some difficulty was experienced in maintaining the belt speed at the free-stream velocity, and these transient indications of boundary layer wedge formation may have been associated with belt speed significantly below free-stream velocity. Also, with the belt running, significant unsteadiness of the boundary between the ground vortex flow field and the free stream was still observed.

Effect of Velocity Ratio

The forward projection of the ground vortex flow field is determined by the energy of the forward-flowing wall jet on the ground relative to the energy of the free-stream flow close to the ground. Previous investigations of jet-induced effects, both in and out of ground effect and at operating conditions involving compressibility effects and hot jets, have shown that the induced effects are a function of the square root of the ratio of jet dynamic pressure to free-stream dynamic pressure. For the present investigation, where the flow is incompressible

and the jet and free stream are at the same temperature, this ratio reduces to the ratio of jet velocity to free-stream velocity.

Figure 8 shows, as expected, that the forward projection of the flow and the depth of the flow both increase as the ratio of jet to free-stream velocity is increased.

Effect of Inlet Flow

Some concern has been expressed that the sink effect of an inlet located slightly ahead of the ground vortex flow field may tend to pull the ground vortex flow forward and aggravate the tendency to ingest hot gas. Similarly, with the inlet slightly above the ground vortex flow field there may be a tendency for the sink effect to raise the upper boundary of the ground vortex flow field. Neither of these effects were observed in the tests. The photographs in figure 8 show comparisons of the flow field with and without inlet flow for two velocity ratios. At a velocity ratio of $V_j/V_0 = 9.1$ the forward projection of the flow field appears to actually be less with the inlet operating. At a velocity ratio of $V_j/V_0 = 11.4$ the ground vortex flow field appears to be deeper and further forward with inlet flow than without. However, these differences are within the scatter caused by the unsteadiness of the boundary between the ground vortex flow field and the free stream. Careful examinations of other photographs and, in particular, review of the video records indicate that the effects of inlet flow on the ground vortex flow field are negligible.

Unfortunately, during the phase I tests it was not always possible to have the inlet mass flow equal to the jet mass flow with the equipment available; but for those operating conditions where the inlet and exit mass flow could be matched, the effects on the ground vortex flow field, if any, were lost in the unsteadiness of the boundary layer between the ground vortex flow field and the free stream, and no effect of varying the inlet mass flow could be observed. The negligible effect of the sink effect of the inlet on the depth and forward projection of the ground vortex flow field was confirmed during the phase II tests when full inlet mass flow was simulated.

Effect of Moving Ground Plane

In considering the proper means of simulating the ground plane, two aircraft operating conditions must be considered: (1) an aircraft hovering in a wind and (2) an aircraft taking off or landing with zero wind. If the condition to be simulated is an aircraft hovering in a wind, the fixed ground board approximates the correct flow field. When hovering in a wind, the free stream approaching the aircraft includes a boundary layer between the free stream (wind) and the ground. However, the flow field in the wind tunnel may not exactly match the actual atmospheric flow field because the boundary layer profile normally available in a wind tunnel will probably have less energy deficiency near the ground than the boundary layer present under atmospheric winds. Schwantes (ref. 2) set out to simulate the boundary layer associated with atmospheric winds. His results show more forward projection of the ground vortex flow field than most other studies.

If the condition to be simulated is an aircraft taking off or landing with zero wind, the flow field generated over a conventional fixed ground board is in error on

two counts: First the forward velocity is represented by the flow approaching the model, and this flow includes a boundary layer between the free-stream flow and the fixed ground board; this boundary layer should not be present. The wall jet flowing forward from the jet impingement point can penetrate further upstream against the lower energy in this boundary layer than it could if the full energy of the free stream extended to the ground surface. A properly designed moving-belt ground board includes a boundary layer removal slot ahead of the belt to remove the free-stream boundary layer, and the belt, moving at the same speed as the free stream, prevents this boundary layer from redeveloping (left side of fig. 9).

Second, the scrubbing action of the ground surface acting on the wall jet under the moving aircraft (or model) causes the wall jet to decay faster than it would over a fixed ground board. Moving the belt at the same speed as the free stream duplicates this scrubbing effect (right side of fig. 9). This scrubbing effect reduces the energy of the wall jet, and it will not project as far forward over a moving belt or with a moving model (or aircraft) as it would over a fixed ground board.

The scrubbing effect of the moving ground surface on the wall jet was observed with zero tunnel speed in the test program, as shown in figure 10. With zero belt speed (and zero tunnel speed) the wall jet moves out radially in all directions (fig. 10(a)). However, with the belt running at about 40 percent of the jet velocity, the wall jet projects only a small distance ahead of the jet impingement point (fig. 10(b)), and the jet flow is soon carried downstream by the belt.

Wall Jet Turbulence

Sketches of the ground vortex and wall jet flows such as figure 1 imply a smooth flow in the wall jet and a steady boundary between the ground vortex flow and the free stream. However, as discussed at the beginning of the Results and Discussion section, the boundary between the free stream and the ground vortex flow is very unsteady. Figure 10 also shows that the wall jet flow is unsteady. With the belt stopped the flow appears to be a series of concentric, ever-expanding (like ripples on a pond when a rock is tossed in), irregular circles. This same unsteadiness is observed in figure 11, which shows laser light sheet sections through the wall jet flow at zero tunnel velocity.

The cause of this unsteadiness is unknown, but during phase I tests it was feared that it may be caused by an unsteady flow from the nozzle. The scale of the turbulence is large with respect to the nozzle diameter, and it was thought that the flow from the nozzle may be pulsing.

The nozzles for the phase II tests were redesigned in an attempt to minimize this problem. As shown in figure 6, the step at the entrance to the large-diameter flow section upstream of the nozzle was replaced by a diffuser section, two screens were added, and a finer and longer honeycomb section was installed. No quantitative measurements of the turbulence of the flow from the nozzle or in the wall jets were made, but the character of the wall jet flow generated by the phase II nozzle did not appear to be different than that generated by the phase I nozzle. This suggests that the unsteady nature of the wall jet flow may be associated with the type of unsteady flow observed in the shear layer of an open jet or that the unsteady flow may be a natural result of impingement and the transformation of the impinging jet into the wall jet.

Forward Projection of Ground Vortex Flow Field

As indicated in the introduction and shown in figure 2, there are large differences in measurements of the forward projection of the ground vortex flow field among several wind tunnel investigations (refs. 1 to 4) and between wind tunnel studies and the moving model investigation (ref. 5). A comparison of the results over the fixed ground board and those over the belt is presented in figure 12. Although there is considerable scatter, the results clearly show less forward projection of the flow field with the belt running at the same speed as the free stream. With the belt moving, the forward projection is in good agreement with the moving model results of reference 5.

Reference 1 presented an expression for estimating the forward projection X of the ground vortex flow field that included the effects of height h, velocity ratio, jet width/length ratio w/ℓ, and jet deflection angle δ. This expression can be written as

$$\frac{X}{d} = \frac{h}{d} \tan (\delta - 90) + 0.75\sqrt{\frac{q_j}{q_0}} \left(\frac{\delta}{90}\right)^2 K$$

$$- 1.75\left(\frac{w}{\ell}\right)_j^{0.3}\left(\frac{q_j}{q_0}\right)^{-1.12} [1 - \sin (\delta - 90)]\left(\frac{h}{d}\right)^{2.5} \left(\frac{\delta}{90}\right)^2 \qquad (1)$$

where d is jet diameter, q_j is jet dynamic pressure, q_0 is free-stream dynamic pressure, K is the moving ground factor, and X is measured from the jet center projected to the ground surface.

The first term accounts for the geometric effect of jet deflection in moving the impingement point forward or aft from the jet center. The second term accounts for the basic effects of velocity ratio as well as for the effect of jet deflection in biasing the amount of the jet flow entering the forward-flowing part of the wall jet. The last term modifies the second term for the aft deflection of the jet stream by the free stream. As the height is increased, the jet impingement point is moved aft by the rearward deflection of the jet due to interaction with the free stream. This moves the entire flow field aft and also reduces the amount of flow going into the forward-flowing part of the wall jet.

Equation (1) is presented in terms of the square root of the ratio of the jet to free-stream dynamic pressure (as it was in ref. 1, which is the source of equation (1)). The square root of the dynamic pressure ratio is used to account for the effects of compressibility and jet temperature. For the present tests where the flow is incompressible and the jet and free-stream flows are at the same temperature, this reduces to the ratio of jet to free-stream velocity, which is used in the data plots presented in this paper.

The factor K is introduced to modify the method of reference 1 to account for the effects of the belt. Figure 12 shows that with the belt operating at the free-stream velocity, a value of K = 0.67 brings the estimate into good agreement with the data. With the belt stopped (K = 1.0) the data from the phase I tests are in reasonably good agreement with the estimate; however, the phase II data depart from the estimate at the higher ratios of jet to free-stream velocity (fig. 12 (b)). The reason for this departure is not known.

The present results suggest that a value of K = 0.67 should be used for takeoff and landing with zero wind. For hover with no wind, the results of reference 2 suggest the possibility that $K \geq 1.0$; for takeoff or landing in a headwind, $0.67 \leq K \leq 1.0$ may be appropriate. However, the present data base does not permit determining the variation of K with the ratio of headwind to takeoff or landing velocity.

Depth of Ground Vortex Flow Field

As indicated in the introduction, few data were available on the depth of the ground vortex flow field. Abbott (ref. 5) merely stated that the depth of the flow field was about one-half the forward projection. Typical Z/d measurements of the present investigation are shown in figure 12. These results are in good agreement with the observation of reference 5. It is interesting that there is no discernable difference between the belt-operating and belt-stopped data. The data (including results for deflected jets, discussed in the following section) indicated that the average depth Z of the ground vortex flow field for vertically impinging jets can be estimated by

$$\frac{Z}{d} = 0.25\sqrt{\frac{q_j}{q_0}}\left(\frac{\delta}{90}\right)^2 \qquad (2)$$

Effect of Jet Deflection

When the jet impinges on the ground vertically, the flow outward from the impingement point is equal in all directions. If the jet impinges at an angle, the flow is asymmetrical. A forward-projected jet (as for thrust reversers) should project the ground vortex flow field further forward, and a rearward-deflected jet should reduce the forward projection of the flow field. These observations are born out in the photographs shown in figure 13.

The forward projection and depth of the ground vortex flow field for 120° and 60° jet deflections are presented in figure 14. The forward projection, estimated by equation (1), is in reasonable agreement with the experimental data, but there appears to be no noticeable effect of the belt. Both the belt-running and the belt-stopped data for the 120° deflection agree with the estimate for the belt-stopped case; for the 60° case, both the belt-running and belt-stopped data agree with the estimate for the belt-running case.

As expected, the depth of the flow field is greater for forward deflections and less for aft deflections. It appears that these effects are proportional to the square of the deflection angle.

Side-by-Side Jets

At zero forward speed (in hover), the wall jets from two jets will meet between the jets and form an upwash fountain flow. If jets are side by side with respect to the free-stream direction, this fountain will be aligned with the free-stream direction, and for closely spaced jets, a forward projection of the flow would be expected

at forward speed. However, if the jets are far enough apart, they will act as individual jets at relatively high forward speeds, and the forward-projecting part of the fountain will not appear until low speeds (high ratios of jet to free-stream velocity).

In the present study the ground vortex flow field for side-by-side jets was investigated only for a spacing of 10 diameters. As can be seen in figure 15, at the lowest jet to free-stream velocity ratio (upper left) the two jets are early operating independently. The fountain flow can be seen at zero forward speed ($V_j/V_0 = \infty$, hover) but does not appear until $V_j/V_0 = 9.6$ is achieved and does not project ahead of the jets until $V_j/V_0 = 16.1$.

The forward projection and depth of the flow field for side-by-side jets are compared with those for a single jet in figure 16. Within the range of the data, the jets at this spacing of 10 jet diameters produce forward projections and depths equal to those for a single jet.

Jets in Tandem

With two jets in tandem, the fountain flow generated in hover will be crosswise to the free stream, and the rear jet will be operating in the wake of the front jet. Figure 17 presents photographs of the flow for a jet spacing of 10 diameters. The fountain generated in hover can be seen at the right. This fountain grows rapidly in width as it rises from the ground and, as others have noted, is very unsteady. At high forward speed (low ratio of jet to free-stream velocity, left side of fig. 17), a ground vortex is formed ahead of each jet. As can be seen in figure 18(a) both of these ground vortices have the characteristic horseshoe shape. As the jet to free-stream velocity ratio is increased, the rear ground vortex moves forward until it reaches the midpoint between the jets, and a straight-across fountain flow is generated (fig. 18(c)).

The forward projection of the ground vortex flow field generated by the front and rear jets is compared with the same quantities generated by a single jet in figure 19. For the wide spacing (10 diameters, fig. 19(a)) and the belt running, the ground vortex flow field generated by the front jet is essentially the same as that generated by the single jet. However, as expected, the flow field created by the rear jet only progresses forward to the fountain position. The slightly more forward position shown by the data points in figure 19 is due to the width of the fountain flow.

With the belt stopped (fig. 19(b)), the flow field generated by the front jet does not progress as far forward as that of an isolated jet. In fact the flow field only progresses as far forward as it would with the belt operating at free-stream velocity. This appears to be true for both the wide (fig. 19(b)) and close (fig. 19(c)) spacing. For the more closely spaced tandem pair, the depth of the ground vortex flow field generated by both the front and rear jets appears to be less than that generated by the single jet. The reason for this behavior is unknown.

Effect of Blocking Surface

In an actual airplane the ground vortex flow field may completely fill space below the lower surfaces of the aircraft for some operating conditions. Reference 1 showed that when this occurs, the forward progression of the ground vortex flow field is reduced. Only limited data were obtained for this condition in the present investigation. The data for the tandem pair (fig. 20(a)) agree with the results of reference 1. The depth of the flow field equals the height at $V_j/V_0 \approx 16$, and the forward progression at higher velocity ratios is less than for the front jet without the blocking plate.

With the side-by-side pair, the results are less conclusive. The depth of the flow field again fills the space between the blocking surface and the ground at $V_j/V_0 \approx 16$, but there is only one data point at a higher velocity ratio, and this shows only marginally less forward projection.

CONCLUDING REMARKS

This water tunnel flow visualization of the ground vortex flow field has shown that both the wall jet that generates the ground vortex and the boundary between the ground vortex flow field and the free-stream flow are very unsteady.

The forward projection of the flow field with a fixed ground board generally validates the method of estimating this forward projection presented in reference 1. However, the fixed ground board does not properly simulate the takeoff or landing flow fields. With a moving-belt ground board, which eliminates the boundary layer between the free stream and the ground surface and also introduces the scrubbing action of the ground surface on the wall jet flowing forward from the impingement point, the forward projection of the flow field is only about two-thirds of that measured over a fixed ground board.

The depth of the flow field is proportional to the square root of the ratio of the jet dynamic pressure to the free-stream dynamic pressure and to the square of the jet deflection angle.

The size of the flow field generated by the front jet of a widely spaced tandem pair is the same as that generated by the front jet alone. However, the size of the flow field generated by the front jet appears to reduce as the jets are moved closer together.

Inlet flow did not noticeably affect the forward projection or depth of the flow field.

REFERENCES

1. Stewart, V.R.; and Kuhn, R.E.: A Method for Estimating the Propulsion Induced Aerodynamic Characteristics of STOL (short takeoff and landing) Aircraft in Ground Effect, vol. 1. NADC-80226-60, Aug. 1983.

2. Schwantes, E.: The Recirculation Flow Pattern of a VTOL Lifting Engine. NASA TT-F-14912, 1973.

3. Weber, H.A.; and Gay, A.: VTOL Reingestion Model Testing of Fountain Control and Wind Effects. Eleventh Propulsion Conference, AIAA-75-1217, Sept. 1975.

4. Colin, P.E.; and Olivari, D.: The Impingement of a Circular Jet Normal to a Flat Surface With and Without Cross Flow. AD-688953, European Research Office, United States Army, Jan. 1969.

5. Abbott, W.A.: Studies of Flow Fields Created by Vertical and Inclined Jets When Stationary or Moving Over a Horizontal Surface. ARC-CP-911, 1967.

6. Beckner, C.; and Curry, R.E.: Water Tunnel Flow Visualization Using a Laser. NASA TM-86743, 1985.

7. Cimbala, J.M.; Stinebring, D.R.; Treaster, A.L.; and Billet, M.L.: An Experimental Investigation of a Jet Impinging on a Ground Plane in the Presence of a Crossflow. NADC-87019-60, March 1987.

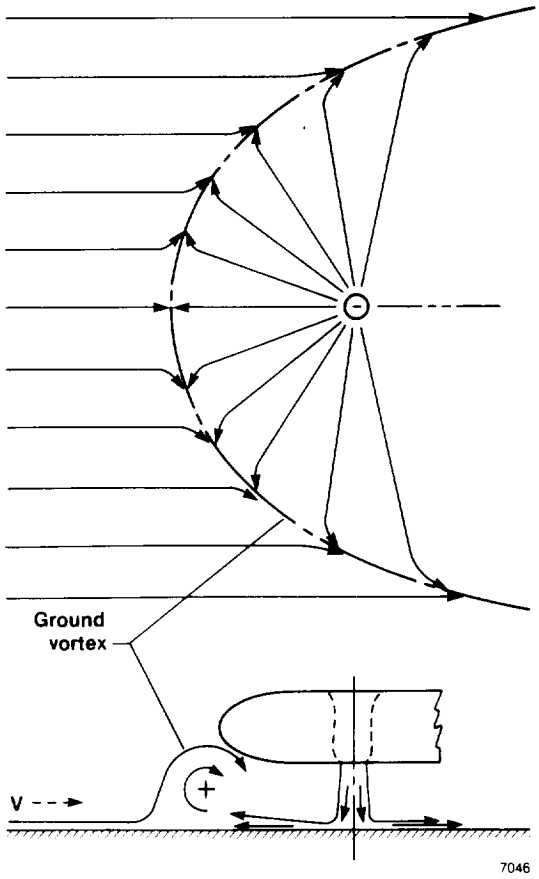

Figure 1. Formation of the ground vortex flow field.

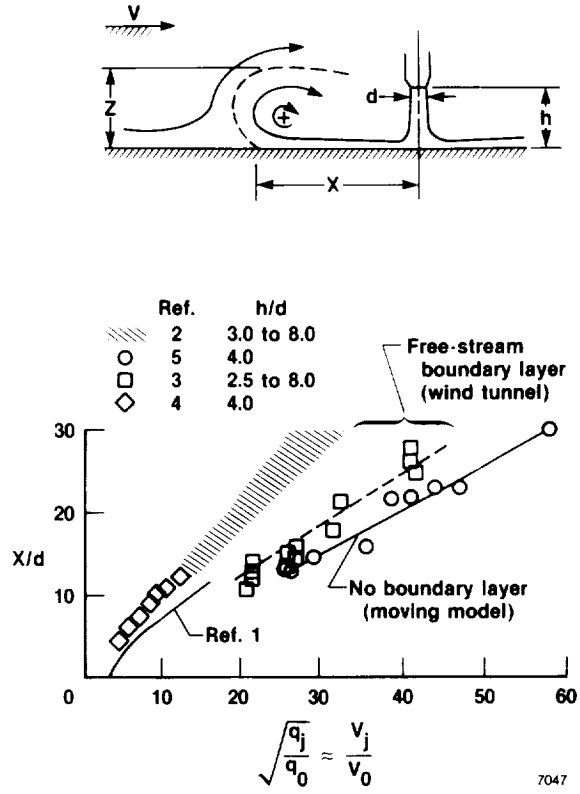

Figure 2. Forward projection of the ground vortex flow field as determined by several investigations.

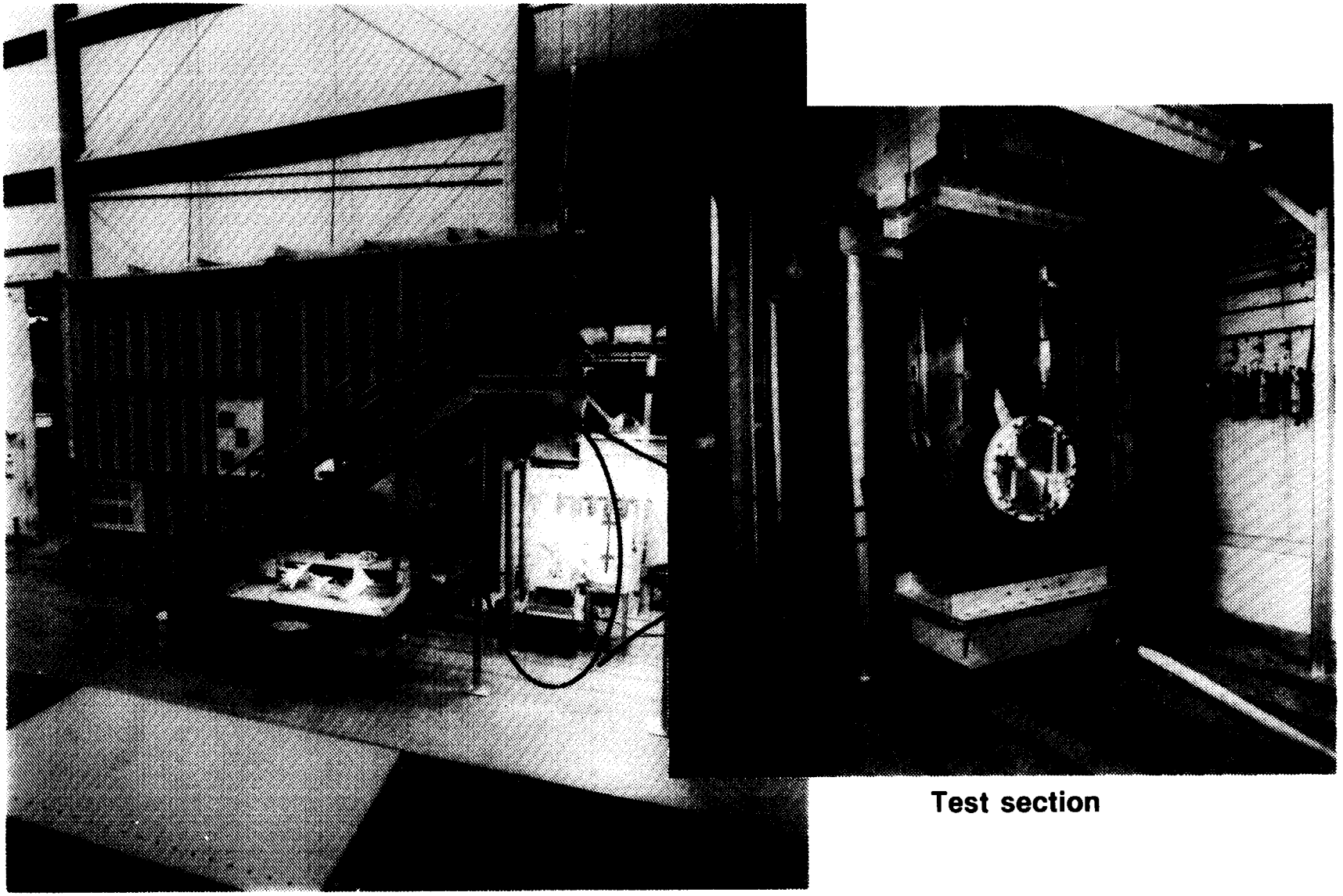

Figure 3. NASA Ames-Dryden Flow Visualization Facility.

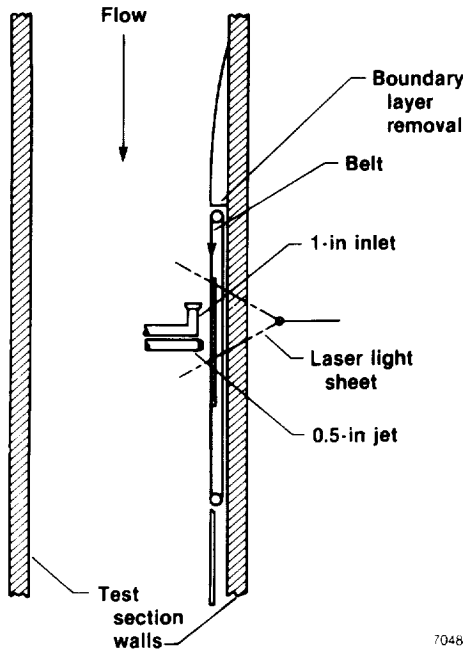

Figure 4. Installation of jet, inlet, and moving ground board in the test section.

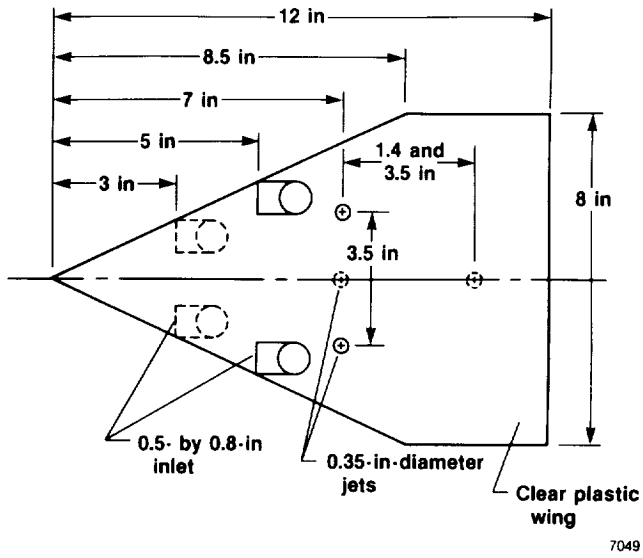

Figure 5. Phase II model.

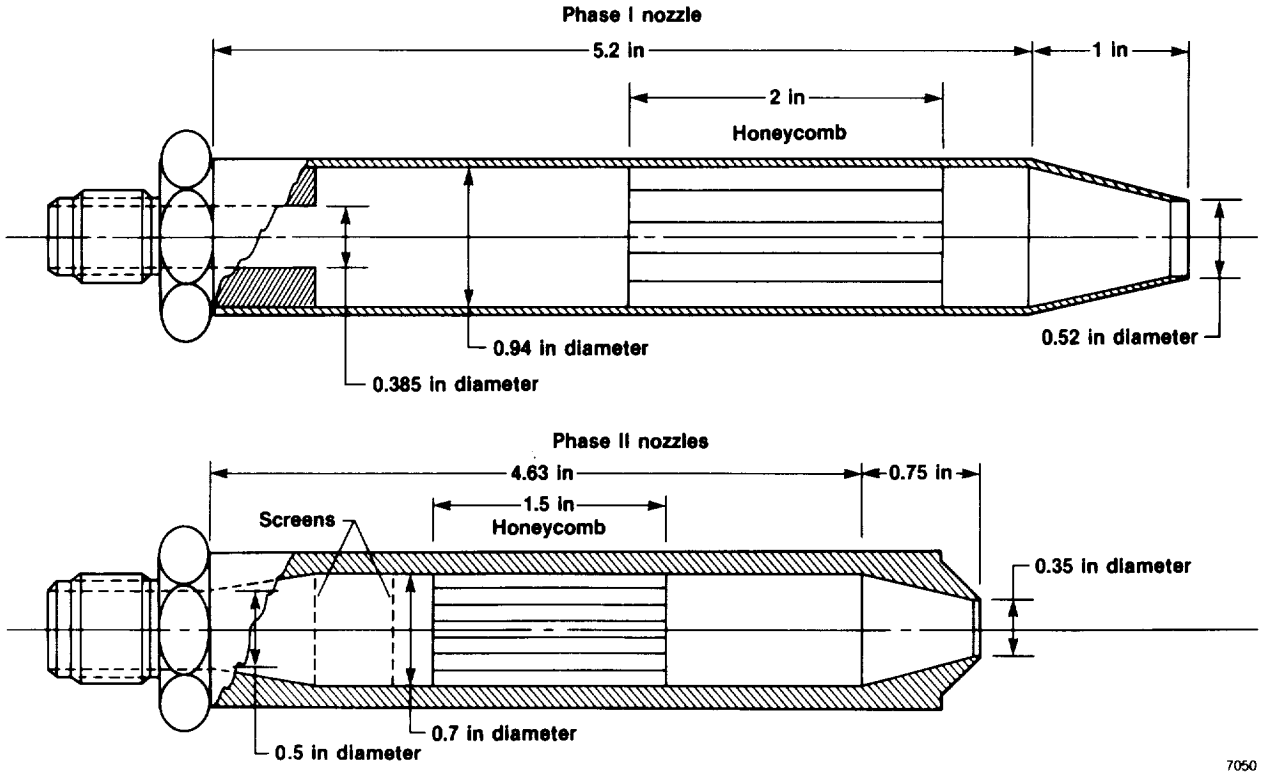

Figure 6. Flow conditioning treatment for phase I and phase II jets.

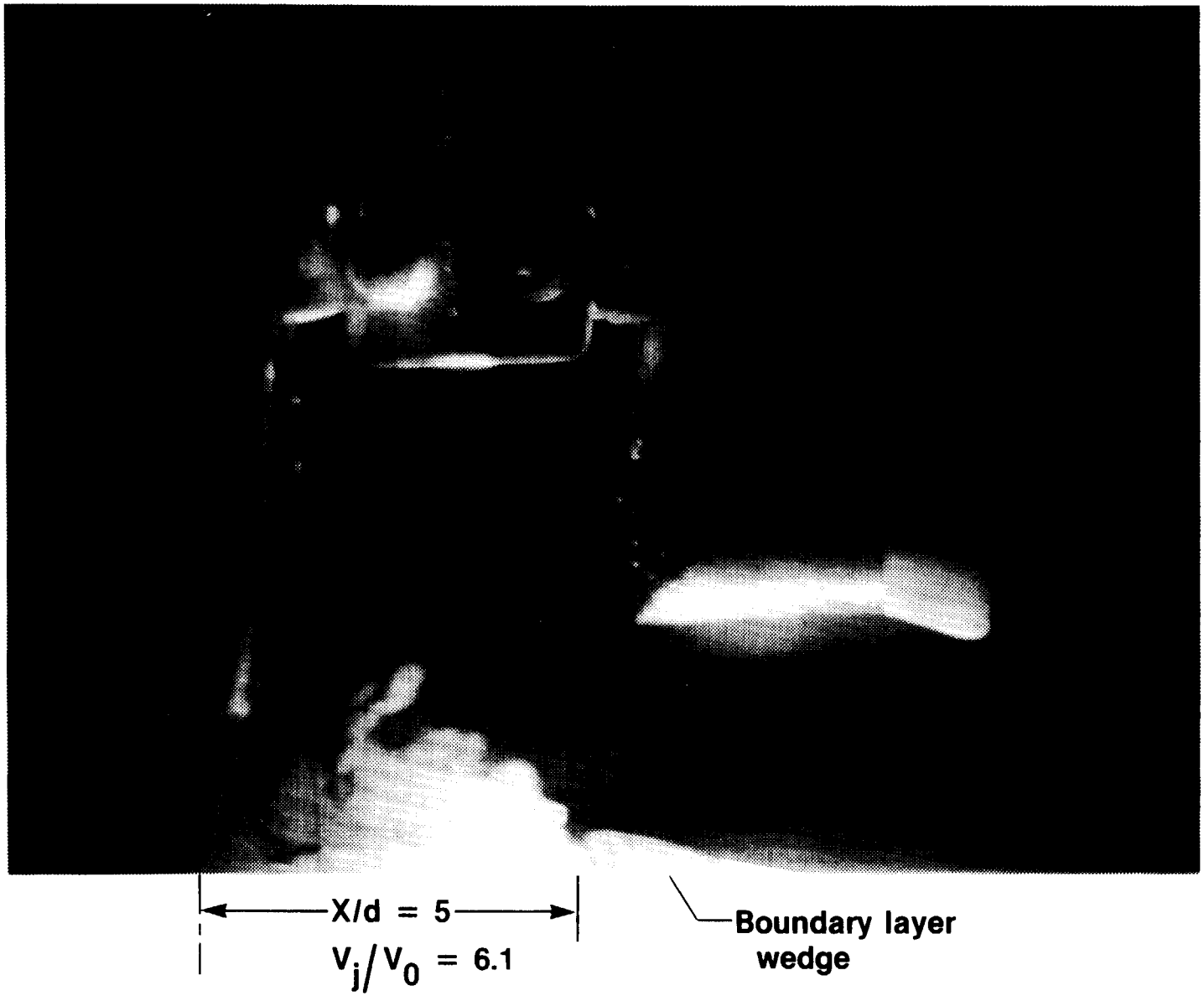

Figure 7. Experimental setup showing jet, inlet, ground vortex flow field, and boundary layer wedge; belt stopped.

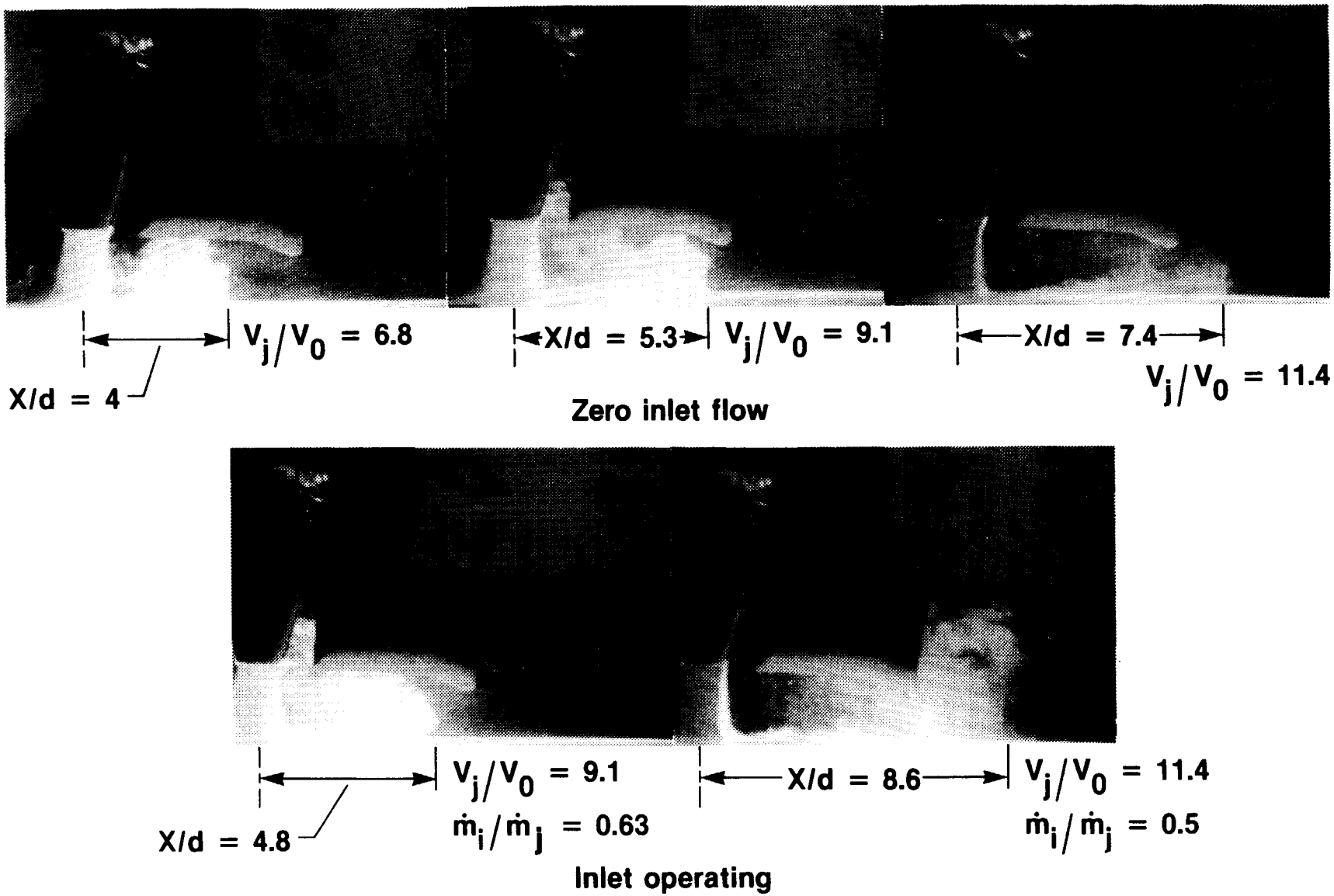

Figure 8. Effect of velocity ratio and inlet flow on forward projection and depth of the ground vortex flow field; h/d = 2, belt running.

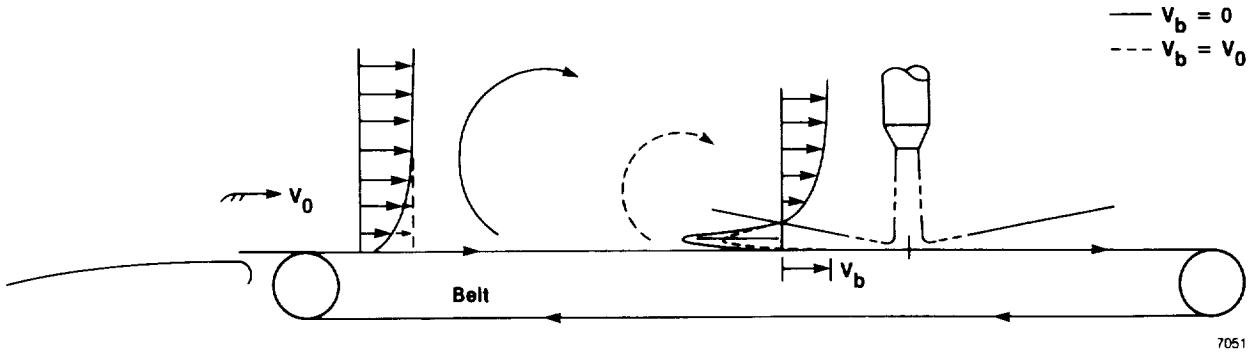

Figure 9. Effect of belt on free-stream flow, wall jet flow, and ground vortex position; V_b is belt velocity.

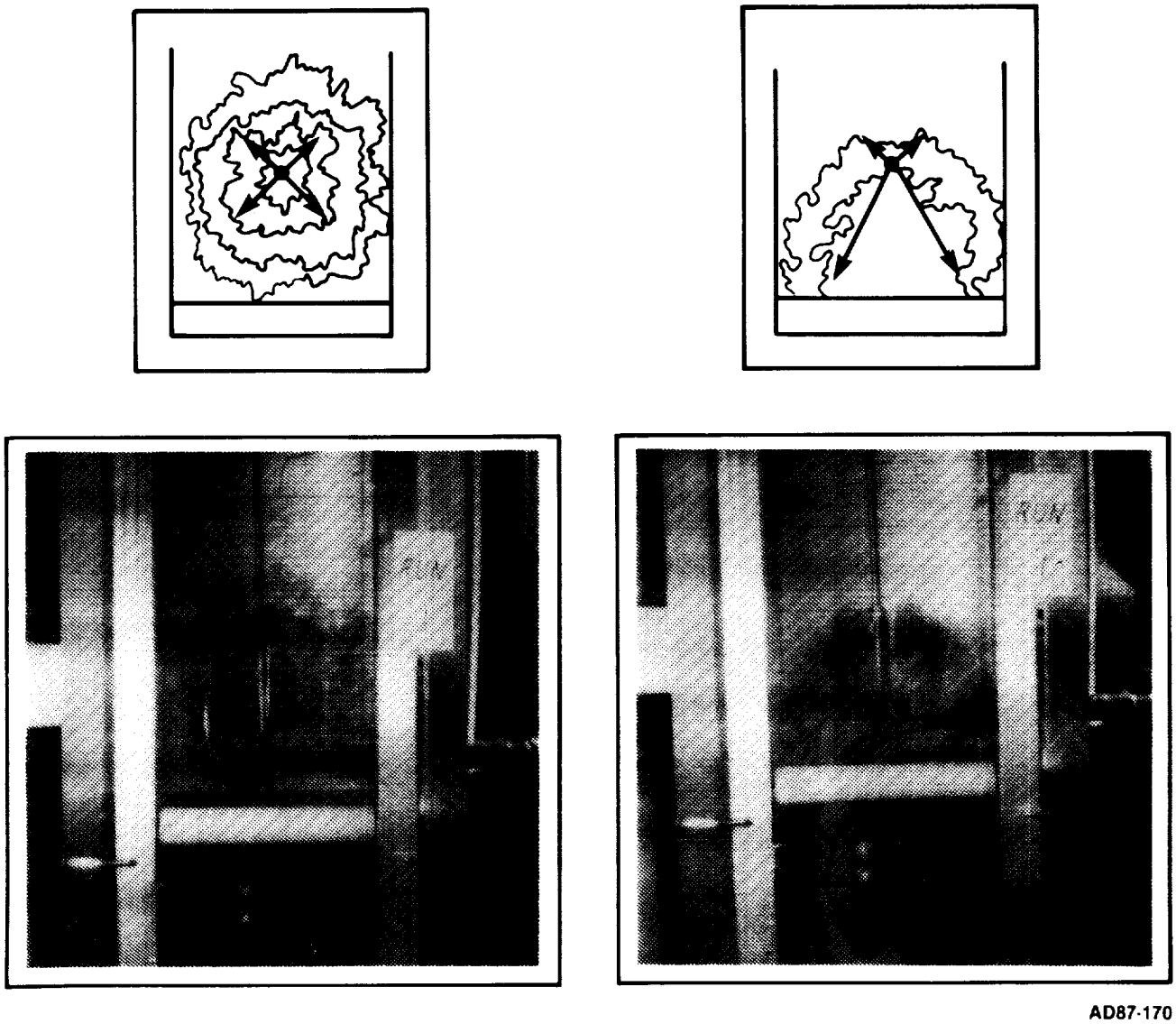

(a) Belt stopped. *(b) Belt running; $V_b = 0.4V_j$.*

Figure 10. Bottom view of wall jet flow at zero tunnel speed (hover).

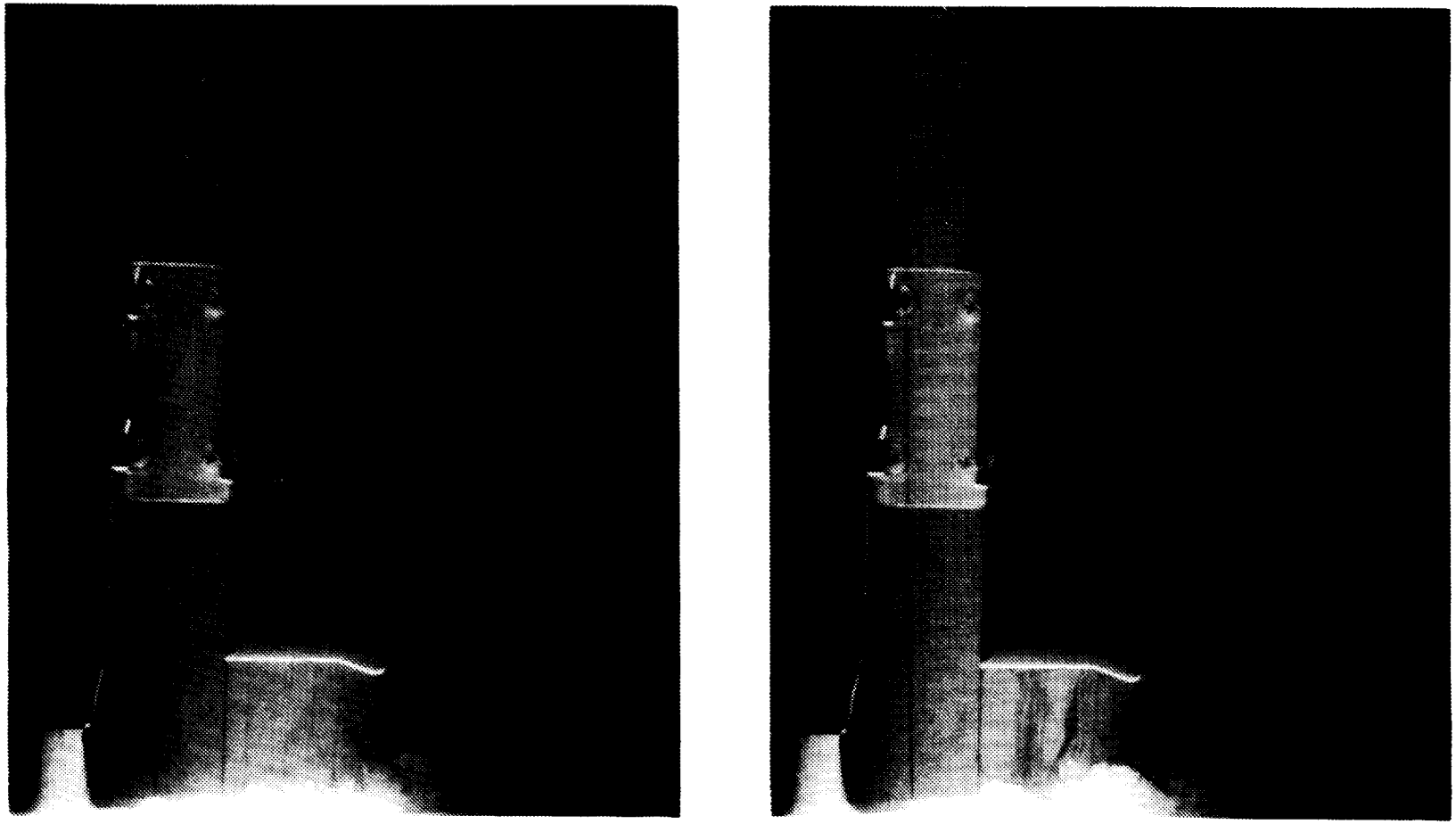

AD87-178

Figure 11. Laser light sheet view of wall jet at zero tunnel speed. The two photographs show the unsteady nature of the flow.

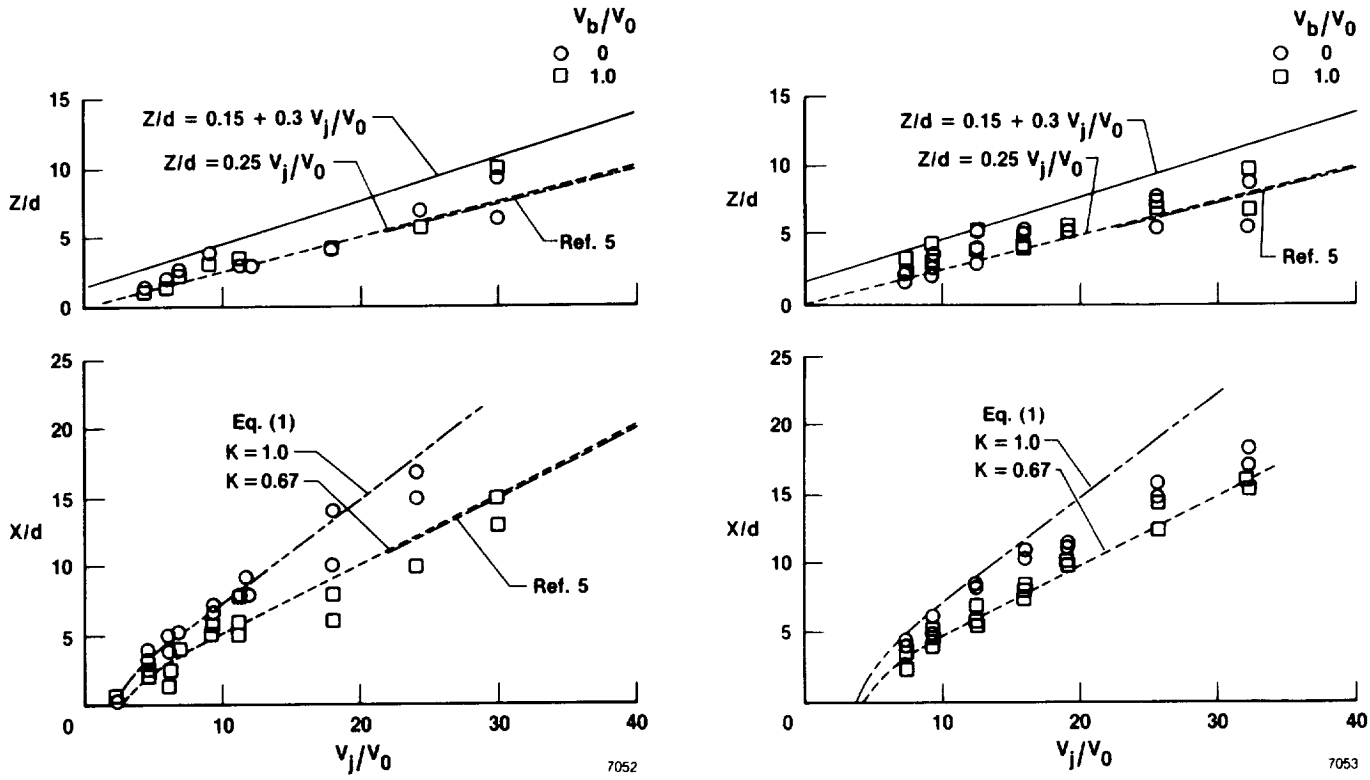

(a) h/d = 2 (phase I). *(b) h/d = 4 (phase II).*

Figure 12. Effect of velocity ratio and belt speed on forward projection and depth of the ground vortex flow field.

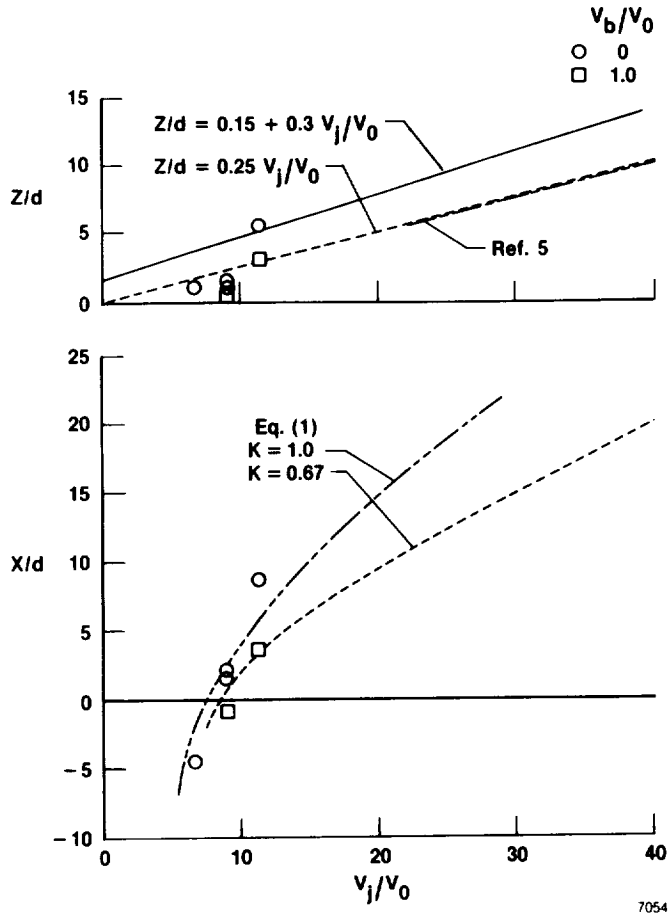

(c) h/d = 10 (phase I).

Figure 12. Concluded.

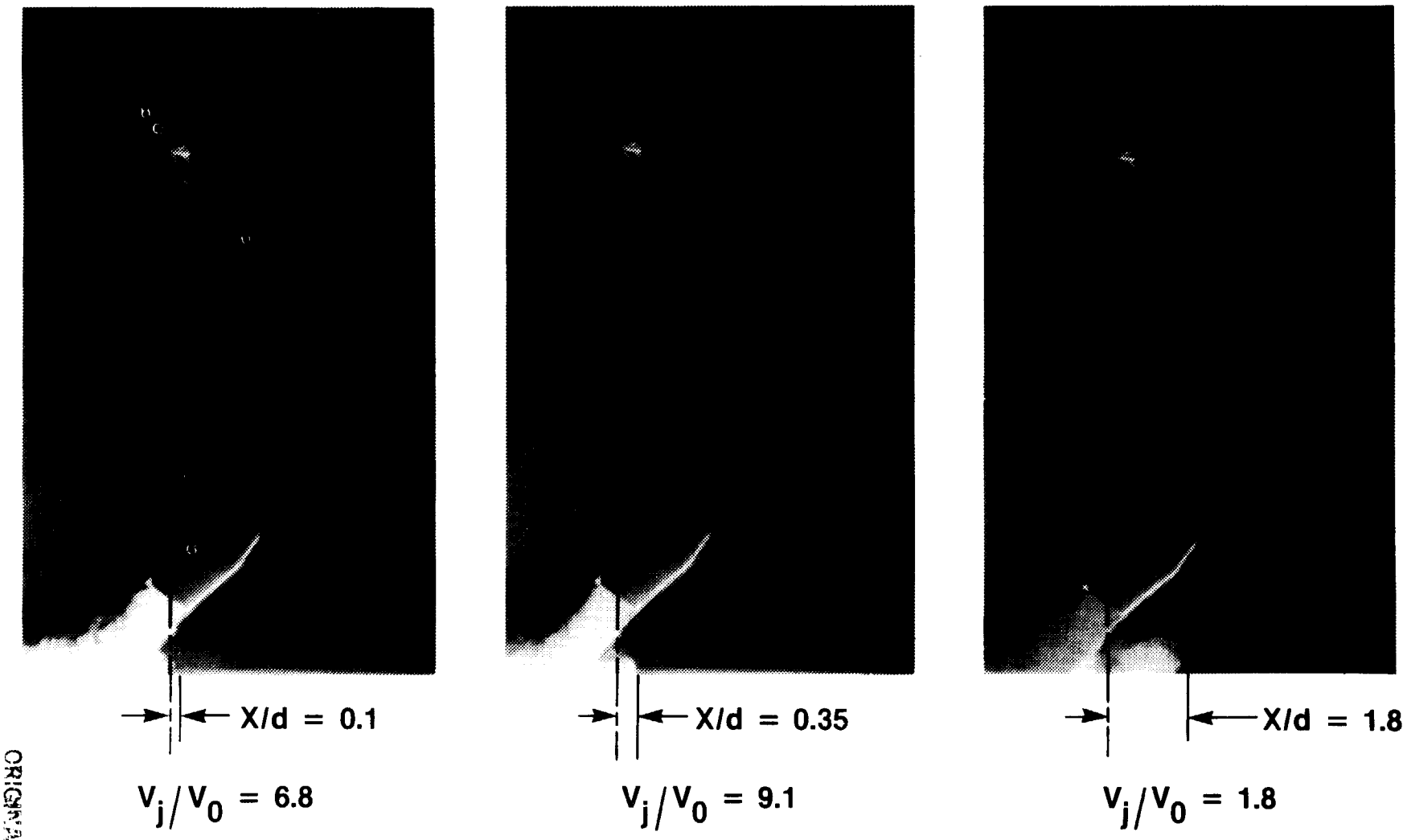

(a) δ = 60°.

Figure 13. Flow field with jet deflected; belt running.

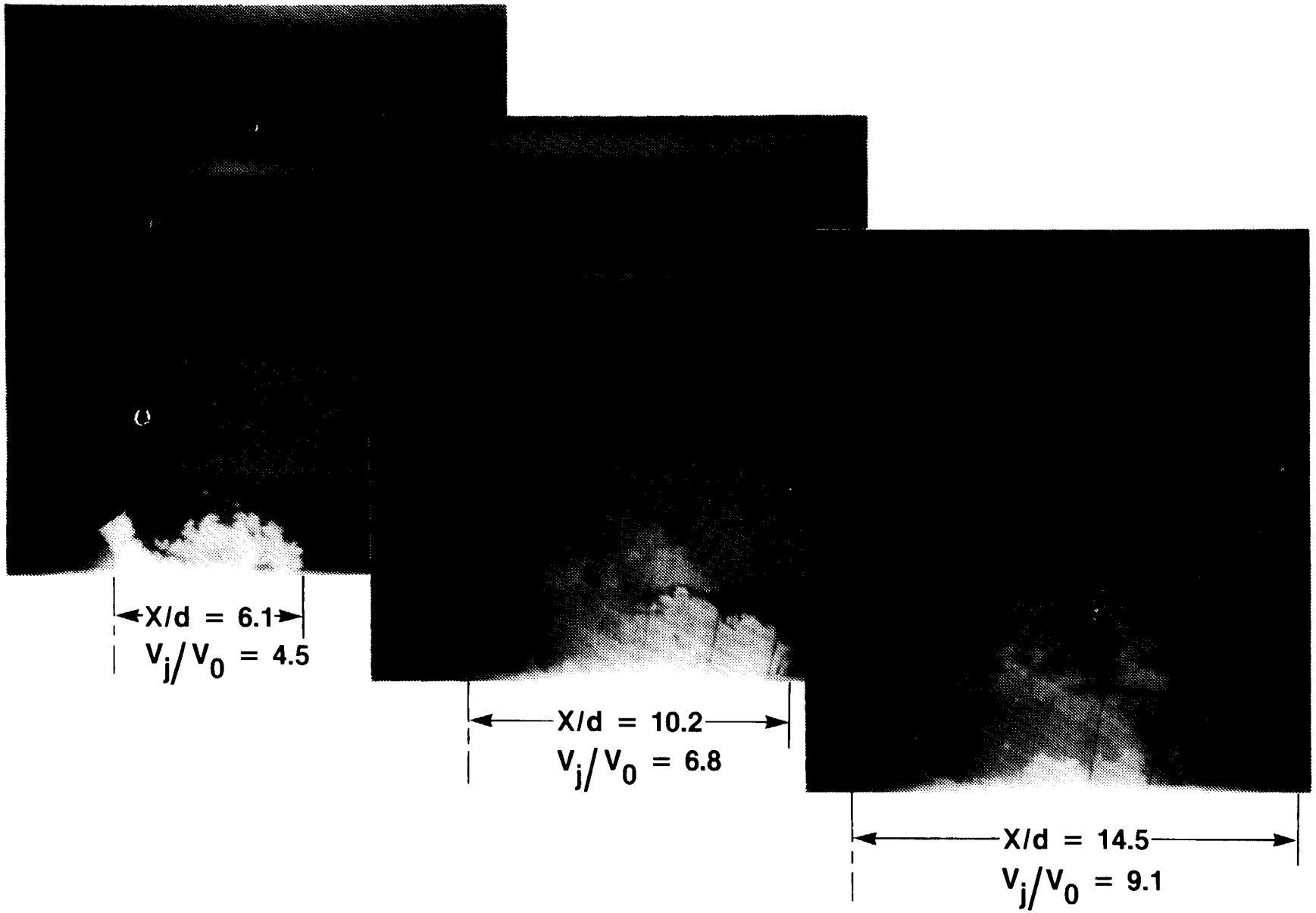

(b) δ = 120°.

Figure 13. Concluded.

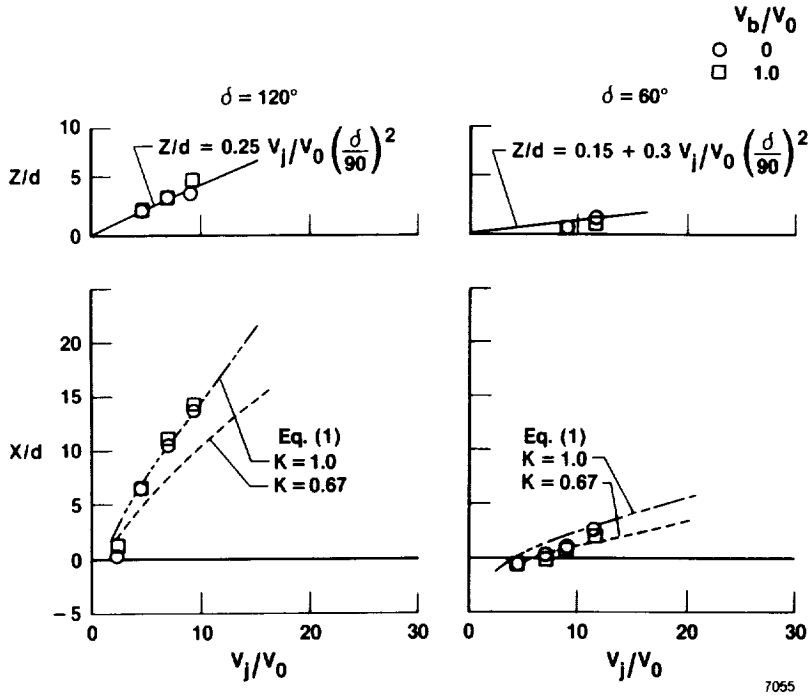

Figure 14. Effect of impingement angle on flow field size; h/d = 2.

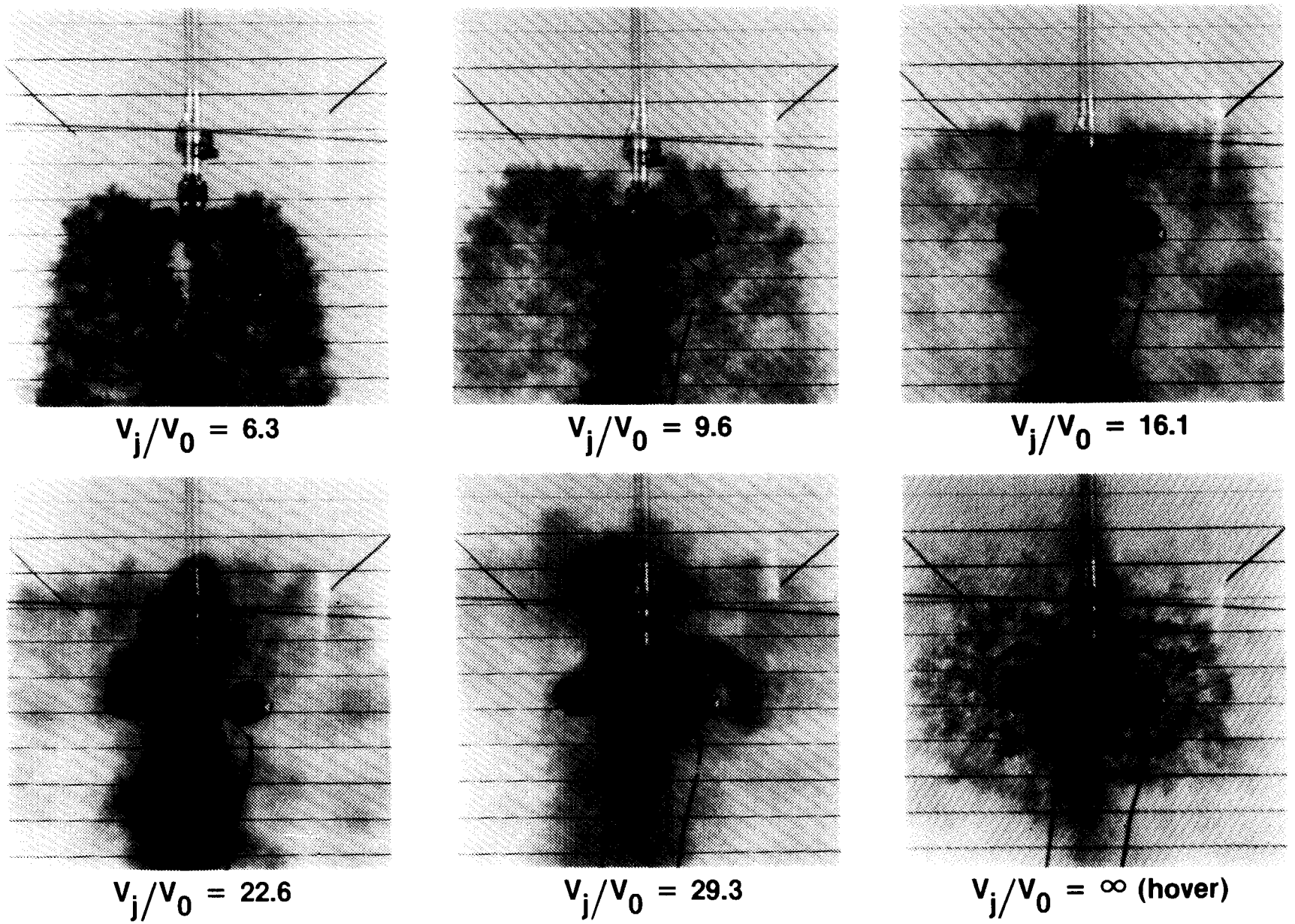

Figure 15. Bottom view of ground vortex flow fields generated by side-by-side jets.

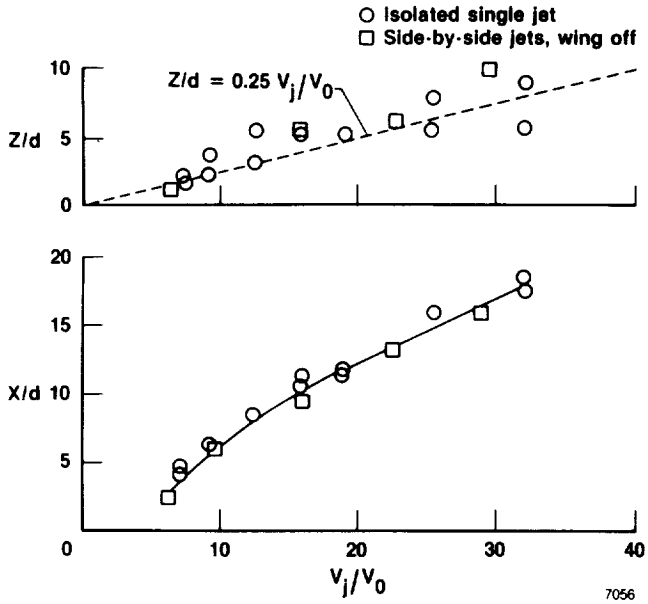

Figure 16. Comparison of sizes of flow fields generated by an isolated jet and side-by-side jets.

(a) V_j/V_0 = 6.3.

(b) V_j/V_0 = 16.1.

AD87-169

(c) V_j/V_0 = ∞ (hover).

Figure 17. Laser light sheet view of flow fields generated by tandem jets; X/d = 10.

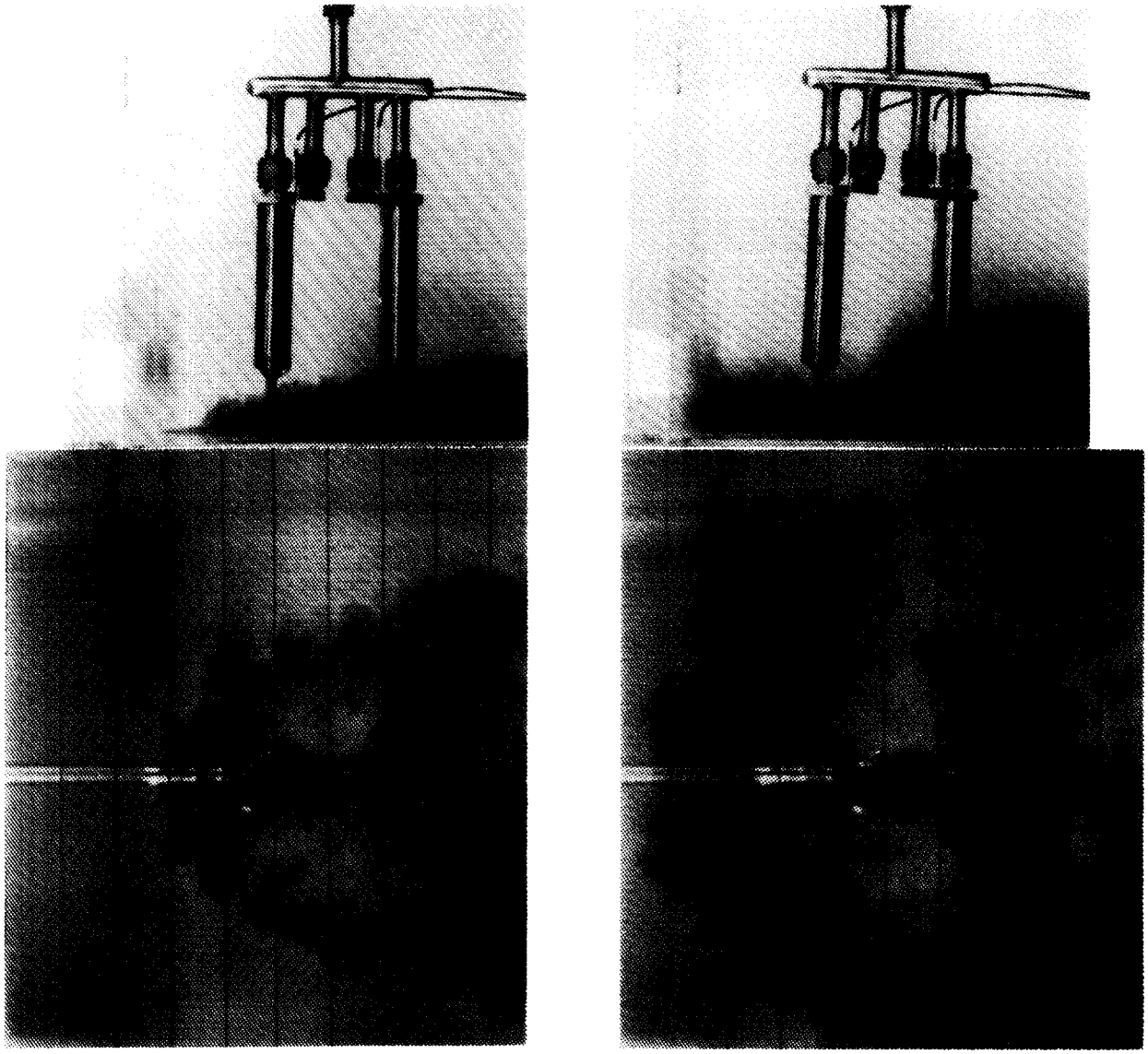

Figure 18. General lighting view of flow fields generated by tandem jets; X/d = 10.

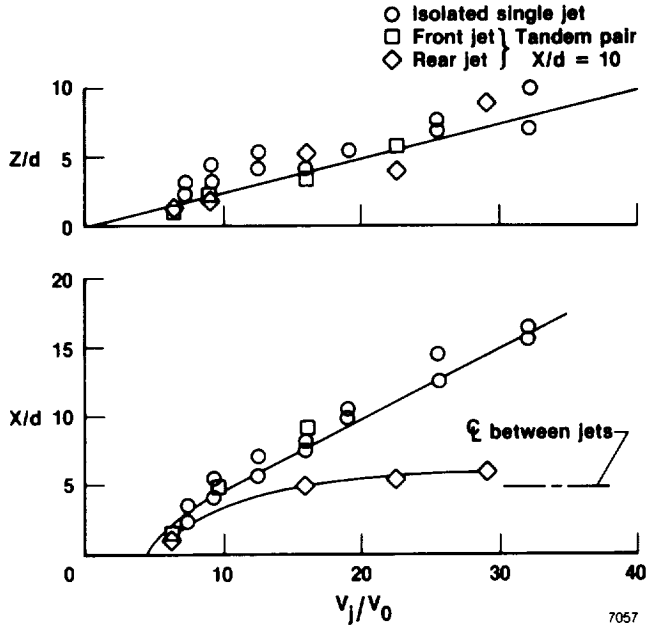

(a) Wide spacing, X/d = 10, belt running.

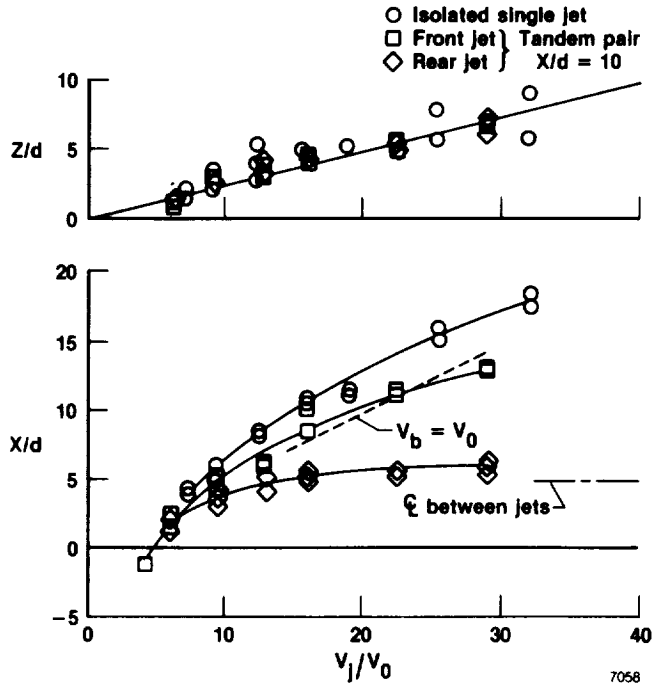

(b) Wide spacing, X/d = 10, belt stopped.

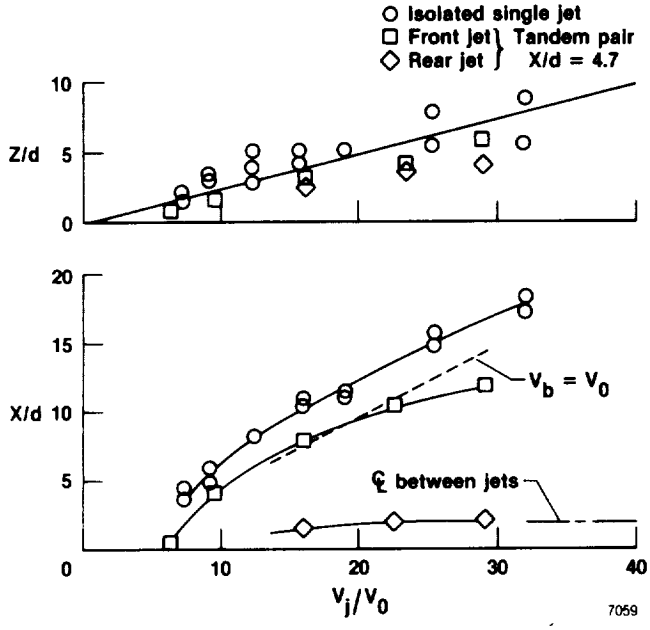

(c) Close spacing, X/d = 4.7, belt stopped.

Figure 19. Comparison of sizes of flow fields generated by an isolated jet and front and rear jets of a tandem pair.

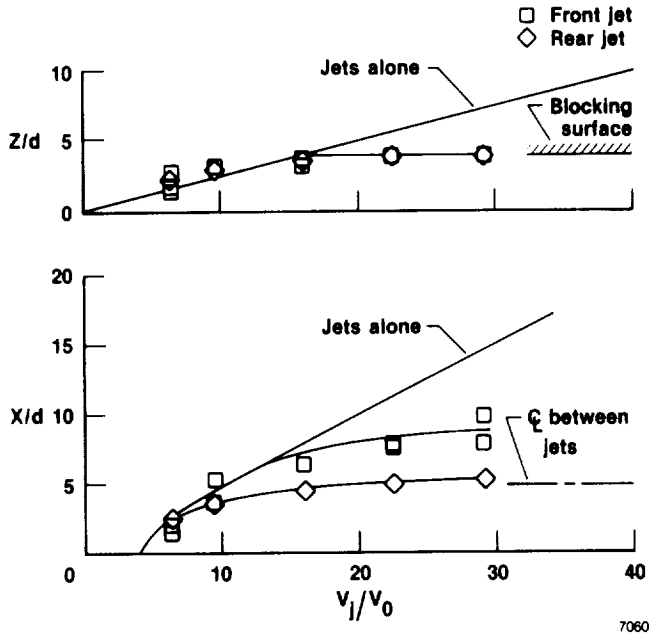

(a) Tandem jets.

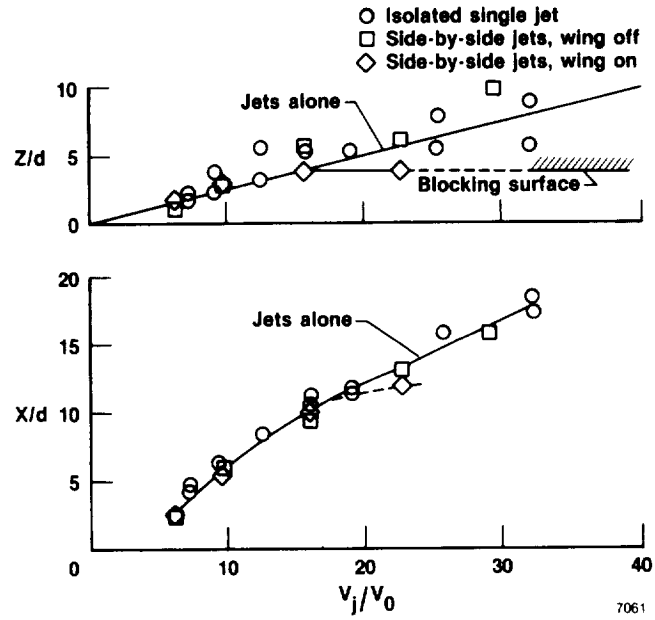

(b) Side-by-side jets.

Figure 20. Effect of a blocking surface on flow field size.